REVIEW

Check for updates

Organic and inorganic nanomedicine for combination cancer therapies

Donghyun Lee,[†a] Jeongsu Shin, [ID][†a] Hangyu Son, [ID][a] Seo Young Cheon,[a] Yeeun Lee,[a] Joonhyuck Park [ID] [*a] and Heebeom Koo [ID] [*ab]

In many cases, a single mode of cancer therapy shows limited efficacy in treating complex and heterogeneous tumors. To improve cancer treatment, combining chemo-, photodynamic-, photothermal-, radio-, and immunotherapy is clinically recognized. When different therapeutic treatments are combined, they often show synergetic effects that further improve therapeutic outcomes. In this review, we introduce nanoparticle (NP)-based combination cancer therapies that use organic and inorganic NPs. Liposomes, polymers, and exosomes can be prepared with amphiphilic properties, high physical stability, and low immune response to treat cancers in a multimodal way. Inorganic NPs, including upconversion, plasmonic, and mesoporous silica NPs, have emerged as a new technology for photodynamic-, photothermal-, and immunotherapy. These NPs can simultaneously carry multiple drug molecules and deliver them efficiently to tumor tissue, as demonstrated in many studies. In addition to reviewing recent advances in organic and inorganic NPs used in combination therapy for cancers, we also discuss their rational design and the outlook for future nanomedicine development.

[a]Department of Medical Life Sciences and Department of Biomedicine & Health Sciences, College of Medicine, The Catholic University of Korea, 222 Banpo-daero, Seocho-gu, Seoul, 06591, Republic of Korea. E-mail: hbkoo@catholic.ac.kr; joonpark@catholic.ac.kr

[b]Catholic Photomedicine Research Institute, College of Medicine, The Catholic University of Korea, 222 Banpo-daero, Seocho-gu, Seoul, 06591, Republic of Korea

† These authors contributed equally to this work.

1. Introduction

Nanoparticles (NPs) are an attractive topic for biomedical researchers because they can be powerful carriers of drugs and genes.[1] At several tens to hundreds of nanometers, they are larger than small chemicals, proteins, and genes and can carry those molecules. At the same time, they are smaller than and can bind or enter cells. They also can be injected into the human body without clogging conventional syringe needles. Therefore, various NP formulations have been developed as nanomedicines, and some of them have been approved for human use by the US Food and Drug Administration (FDA) and are clinically available (Table 1).[2] For example, the COVID-19 vaccines from Moderna and Pfizer/BioNTech are lipid nanoparticles that contain mRNA, which is a representative example of nanomedicine.[3]

NPs are particularly advantageous for tumor-targeted drug delivery. After intravenous (i.v.) injection, they can provide longer blood circulation than small molecules. The enhanced

Donghyun Lee obtained his B.S. from Hallym University in 2018. He is now a Ph.D. student under the supervision of Prof. Heebeom Koo in the Department of Biomedicine & Health Sciences at The Catholic University of Korea. He completed two projects for tumor-targeted photodynamic therapy, and his current research focuses on heart-targeted drug delivery systems.

Jeongsu Shin obtained his B.S. from Kangwon University. Currently he is a graduate student under the supervision of Prof. Joonhyuck Park in the Department of Biomedical and Health Sciences at The Catholic University of Korea. His research interests are focused on drug delivery systems and biosensors.

Table 1 A list of representative commercially available nanoparticles

Name	Drug	Formulation	Approval	Administration	Application
Abraxane	Paclitaxel	Albumin NP	USA (2005)	Intravenous	Cancer
Doxil	Doxorubicin	Liposome	USA (1995)	Intravenous	Cancer
Feraheme	N/A	Polymer-coated iron oxide NP	USA (2009)	Intravenous	Anemia
Feridex I.V.	N/A	Dextran-coated iron oxide NP	USA (1996)	Intravenous	MRI contrast agent
Genexol PM	Paclitaxel	Polymeric micelle	Korea (2007)	Intravenous	Cancer
Marqibo	Vincristine	Liposome	USA (2012)	Intravenous	Leukemia
Mepact	Mifamurtide	Liposome	Europe (2009)	Intravenous	Osteosarcoma
SPIKEVAX	mRNA	Lipid NP	USA (2022)	Intramuscular	Covid-19 vaccine
COMIRNATY	mRNA	Lipid NP	USA (2021)	Intramuscular	Covid-19 vaccine
Nano Therm	N/A	Iron oxide NP	Europe (2010)	Intratumoral	Cancer
Onivyde	Irinotecan	Liposome	USA (2015)	Intravenous	Cancer
ONPATTRO	siRNA	Lipid NP	USA (2018)	Intravenous	Polyneuropathy
VISUDYNE	Verteporfin	Liposome	USA (2000)	Intravenous	Macular degeneration

permeability and retention (EPR) effect of NPs means that they efficiently accumulate in angiogenic tissue such as tumors by penetrating fenestrated blood vessels and reducing lymphatic drainage.[4] Modifying the surfaces of NPs with biological ligands such as antibodies, aptamers, or peptides can increase their binding to specific receptors on target disease cells.[5] Rationally designed structures responsive to stimuli such as pH, heat, enzymes, or light can also enhance the efficacy of cargo delivery to tumor tissue.[6] Various NPs using those strategies have demonstrated promising antitumor results, and those approaches have been well summarized in other review papers.[7–9]

For a long time, researchers have been seeking effective anticancer treatments. However, despite remarkable progress, cancer is difficult to cure completely, especially using a single treatment method. Therefore, the importance of combination therapy is increasing, and cocktail formulations of different therapeutic molecules have frequently been tried.[10] In this context, NPs are attractive because they can carry and deliver multiple drugs to target tissues and cells simultaneously, increasing the convenience of combination therapy compared to separate administrations of two or more treatments.[11] In this review, we discuss recent studies that have used NPs to deliver two or more drugs/genes for combination tumor therapy. The studies are categorized as those using organic NPs (liposomes, polymer NPs, and exosomes) and those using inorganic NPs
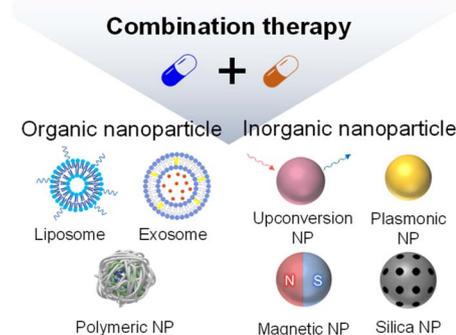
Scheme 1 Organic and inorganic NPs for combination therapy.

Joonhyuck Park received his B.S. and Ph.D. in chemistry from Pohang University of Science and Technology (POSTECH) and trained as a postdoctoral researcher at University of California, Los Angeles (UCLA) and University of Illinois at Urbana-Champaign (UIUC). Now, he is an assistant professor at the Department of Medical Life Sciences in the College of Medicine, The Catholic University of Korea. His research goal is developing nanomaterials that can be applied to therapy and imaging. He is interested in nanocrystals with new optical/physical/chemical properties and their applications at the nano-bio interfaces.

Heebeom Koo received his B.S. and Ph.D. in chemistry from Seoul National University (SNU) and trained as a postdoctoral researcher at the Korea Institute of Science and Technology (KIST) and Massachusetts General Hospital (MGH)/ Harvard Medical School (HMS). Now, he is a professor at the Department of Medical Life Sciences in the College of Medicine, The Catholic University of Korea. His research goal is developing biomaterials that can be applied to therapy. He is interested in nanoparticles and hydrogels with new functions.

(upconversion NPs, plasmonic NPs, and mesoporous silica NPs) (Scheme 1). In particular, we focus on studies containing promising animal data beyond fabrication of NPs or cell experiments.

2. Organic NP-based combination therapy

2.1. Liposomes and phospholipid NPs

A liposome is a traditional and representative nanomedicine with a long history.[12] It is based on phospholipids, which are the main components of biological membranes. Because phospholipids form a bilayer in aqueous conditions due to their amphiphilic structure, a liposome contains both hydrophobic and hydrophilic parts, which makes it a suitable carrier for drug combinations (Table 2). Recently, Park et al. reported a pH-sensitive liposome system that can simultaneously load small-molecule drugs with different physical properties.[13] These liposomes were loaded with hydrophilic doxorubicin (DOX) in the core and hydrophobic pheophorbide a (Pba) in the lipid membrane to deliver a combination of chemotherapy and photodynamic therapy (PDT). Pba is a photosensitizer that can produce cytotoxic reactive oxygen species (ROS) when exposed to a specific wavelength of light. The generated ROS destroy the surrounding cancer cells. ROS generation is also widely used in cancer treatment as a combination therapy with chemotherapy drugs to minimize side effects by reducing drug doses and to maximize therapeutic efficacy. For efficient delivery of drugs to a subcellular target site, Park et al. fabricated a pH-sensitive structure using DOPE (1,2-dioleoyl-sn-glycero-3-phosphoethanol-amine) and Tos (D-alpha-tocopheryl succinate) for selective release of the drugs under acidic conditions, such as those found in tumor tissue. In neutral pH conditions, repulsion between a carboxylic acid group of Tos and a phosphate group of DOPE maintains a lamellar structure, whereas in an acidic environment, protonation of Tos results in aggregation of the lipid head group, leading to dissociation of the

liposome. In their experiments, about 57.99% of the DOX was selectively released from the pH-sensitive liposomes (pH-lipo-DOX-Pba) at pH 5.5, and almost no DOX was released at neutral pH. After cellular uptake, both drugs were successfully delivered to their subcellular target compartments, the nucleus and cytoplasm for DOX and Pba, respectively, producing an excellent tumor-cell killing effect in the 4T1 breast cancer cell line. Furthermore, the liposomes had high tumor accumulation via the tumor-targeting effect of cRGD (cyclic Arg–Gly–Asp) added to their surfaces, and the combination therapy they enabled showed excellent tumor suppression in a 4T1 tumor allograft model. This result indicates that liposomes are an attractive carrier for combination therapies of hydrophobic and hydrophilic drugs.

In addition to being able to carry multiple small molecules, the large hydrophilic cavity of a liposome enables encapsulation of proteins with high molecular weights. Wu et al. reported a liposome that co-delivered a protein and small molecules for effective inhibition of cancer metabolism.[14] They described a glucose oxidase (GOx)- and telaglenastat (Tel)-loaded liposome (Lip@GOx&Tel) for repressing both glycolysis and glutamine metabolism, which are essential for cancer progression. Due to compensation, dual inhibition of glycolysis and glutamine metabolism is necessary to thoroughly block cancer metabolism. Wu et al. formulated a cationic liposome using 1,2-dioleoyl-3-trimethylammonium propane to enhance the uptake into cancer cells and then co-loading GOx and Tel in its hydrophilic cavity and lipophilic membrane, respectively. The Lip@GOx&Tel successfully encapsulated 61.5% of GOx and 74.6% of Tel and showed low glycolysis and mitotic ATP levels, indicating that it effectively downregulated cancer metabolism. In addition, the Lip@GOx&Tel showed the highest ROS level among the tested groups because GOx produced H_2O_2, and Tel prevented the synthesis of glutathione. Based on that mechanism, Lip@GOx&Tel showed enhanced anticancer and anti-metastasis effects than free GOx and Tel in 4T1 breast cancer cells. After i.v. injection in a 4T1-tumor model, Lip@GOx&Tel

Table 2 Summary of studies employing organic NP in combination therapy. The tumor suppression rate was calculated as reduction of tumor size in the combination therapy group compared to the control group non-treated

Formulation	Combination	Drug	Tumor cell (mouse)	Tumor suppression rate	Year	Ref.
Liposome	Chemotherapy/PDT	Doxorubicin/pheophorbide a	4T1 (BALB/c) 52.38	47.6%	2022	13
	Enzyme/chemotherapy	Glucose oxidase/telaglenastat	4T1 (BALB/c)	82%	2022	14
Lipid NP	ECM remodeling/PD-L1 silencing	siRNA/CRISPR-Cas9	Liver tumor (transgenic mouse)	92%	2022	16
Polymeric NP	Chemotherapy/PDT	Tirapazamine/pheophorbide a	SCC7 (C3H/HeN)	96%	2021	24
	Chemotherapy/gene therapy	Doxorubicin/pDNA	MDA-MB-231 (nude mouse)	89.3%	2021	25
	Chemotherapy/chemotherapy	Doxorubicin/erlotinib	SCC7 (C3H/HeN)	73.8%	2021	26
Exosome	Chemotherapy/PDT	Doxorubicin/Rose bengal	A20 (BALB/c)	76.8%	2022	28
	Chemotherapy/PDT	Doxorubicin/Al(III) phthalocyanine chloride tetrasulfonic acid	MGC803 (BALB/c nude)	86.6%	2021	29
	Chemotherapy/radiotherapy	Doxorubicin/radioiodine-131	8505c (BALB/c nude)	84%	2022	30

exhibited high accumulation in tumor tissue and reduced tumor growth, with an 82% tumor suppression rate. It also had lower systemic toxicity than free GOx and Tel due to the stable loading and selective delivery of GOx. Those results indicate that liposomes show promise for combination therapies that use protein drugs or small molecules.

Recently, a lipid nanoparticle (LNP) with a structure slightly different from that of a traditional liposome received attention because it uses the amphiphilic structure of a phospholipid to encapsulate genetic materials such as siRNA or mRNA.[15] LNPs containing COVID-19 mRNA have been approved by the FDA and are being widely used, making them a representative nanomedicine for gene drugs. For efficient encapsulation of mRNA, LNPs were formulated with ionizable lipids that are cationic in acidic conditions and neutral at pH 7.4. They have high transfection efficiency and low toxicity in body conditions. Zhang et al. suggested simultaneous delivery of siRNA and CRISPR (clustered regularly interspaced short palindromic repeat)-associated protein 9 (Cas9) mRNA (Fig. 1).[16] Their strategy enhanced gene editing efficiency in cancer therapy by altering the mechanical properties of the tumor microenvironment. They formulated LNPs containing focal adhesion kinase (FAK) siRNA, Cas9 mRNA, and single guide (sg) RNA (siFAK + CRISPR-LNPs) using 5A2-SC8, an ionizable dendrimer lipidoid reported in their previous work. In their system, siFAK plays the crucial role of alleviating the stiff tumor microenvironment by decreasing stress fibers and actomyosins. The plasticity in the tumor extracellular matrix produced by the siFAK enabled facile penetration of Cy5-labeled LNPs throughout an entire 3D-IGORV1 tumor spheroid within only 4 hours. The amplified infiltration of siFAK + CRISPR-GFP-LNPs elevated CRISPR-Cas9 gene-editing efficacy in a HeLa-GFP spheroid by about 7-fold. In line with those in vitro results, siFAK + CRISPR-PD-L1-LNPs showed increased CD8 + T cell infiltration and significant downregulation of PD-L1 expression, producing an efficient antitumor effect and extending survival in a transgenic mouse bearing MYC-driven liver tumors. Thus, their LNP is an appropriate carrier for combination gene delivery.

2.2. Polymer NPs

Polymers are materials or substances with a high molecular weight that are formed by repeated linkage of numerous monomers. Because they have more useful physical properties than single molecules, they have been widely used as medical materials in situations that require high stability or rigidity. Polyethylene glycol (PEG) and poly(lactic-co-glycolic acid) (PLGA) are representative polymers that are FDA-approved for injection into humans and widely used in clinics. Biopolymers such as hyaluronic acids, chitosan, and gelatin are also useful materials for researchers.[17,18] During NP development, polymers have been used as main components by many researchers.[19–23] Recently, Lee et al. described an optimized combination therapy in gelatin NPs that included Pba for PDT and other anticancer drugs (Fig. 2).[24] They first evaluated the combination index (CI) values between Pba and 12 traditional chemical drugs in vitro to determine the best combination. Only the Pba and tirapazamine (TPZ) combination, which showed the highest synergetic effect in vitro, had a CI value <1 up to the ED90 level, presumably because the hypoxic environment caused by PDT is capable of high TPZ activation. After Pba and TPZ were selected as the optimal pair, they were encapsulated into stable NPs using polymers. Pba and PEG were conjugated to gelatin to create an amphiphilic PEG–gelatin–Pba structure, and TPZ was physically loaded into those NPs with an encapsulation efficiency of 59.7% and a final size less than 200 nm. When the biodistribution was observed in SCC7 tumor-bearing mice, high fluorescent intensity in the tumors was observed beginning 3 hours after i.v. injection of TPZ–Pba–NPs, and it was about 4.12 times higher than that in the free Pba group after 24 hours. To evaluate the therapeutic effects of the NPs carrying TPZ and Pba, the prepared formulation was i.v. injected twice into the same murine tumor models at 24 hour intervals, and then the tumor sites were irradiated with a laser. After 14 days of treatment, the laser-irradiated TPZ–Pba–NP group demonstrated the highest tumor suppression effect among groups, with the tumor resolved completely from one of four mice. These findings indicate that polymer NPs containing both TPZ and Pba were an effective combination therapy in vivo.

Another approach to combination therapy, proposed by Liu et al., is a universal platform for gene and drug delivery.[25] Anticancer drugs are commonly used to disrupt and destroy DNA and RNA inside cancer cells. Therefore, a gene's function as a therapeutic agent could be compromised when it is carried
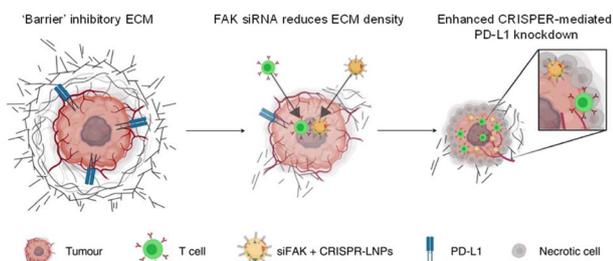

Fig. 1 Lipid NP containing siRNA and a CRISPR formulation for combination gene therapy. Reproduced from ref. 16 with permission from [Springer], copyright [2022].
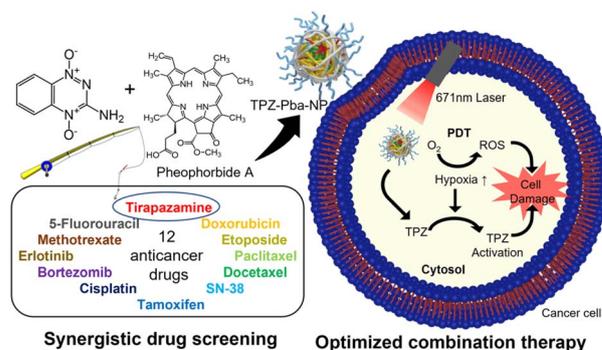

Fig. 2 Gelation NP containing the synergetic pair of tirapazamine and pheophorbide a to combine PDT and chemotherapy. Reproduced from ref. 24 with permission from [American Chemical Society], copyright [2021].

in NPs that also contain anticancer drugs. To address that issue, Liu *et al.* modified calixarene (CA) as a drug container to inhibit activity until transfection, lowering the antagonistic effects of the gene and drug and increasing the therapeutic effect. CA, a molecular drug carrier for the anticancer agent DOX, was modified with azobenzene and carboxyl groups to increase its affinity for hydrophobic molecules and make it responsive to hypoxia. Then, a cationic polyplex core was prepared by mixing phenylboronic acid-modified polyethyleneimine (PEI-PBA) with a plasmid DNA-based CRISPR interference system that targets miR-21. The prepared core was coated with the pH-responsive DOX-CA complex to create the completed particles (CENP-DOX/dCas9-miR-21). When exposed to an acidic tumor environment, the polymer coating on the surface of the polyplex core detached rapidly, exposing the cationic core and leading to high cellular internalization. The modified CA loaded into the core is a key technology that can prevent interaction between therapeutic drugs and genes. It is inactive outside the cell, but when transfected, it is activated by the hypoxic environment inside the cancer cells. The efficacy of the combined treatment was maximized by minimizing interference between the gene and the therapeutic drug, and the excellent antitumor effect was confirmed in animal experiments. For *in vivo* evaluation, tumor-bearing mice were established by subcutaneous injection of MDA-MB231 cells in the mammary fat pad, and all samples were i.v. injected every 5 days. As a result, the combination system demonstrated the highest tumor growth suppression at 89.3%. Thus, a rational design to separate a gene and a drug in the same NP has been shown to be an effective strategy for simultaneous delivery to treat cancer.

In 2021, Lee *et al.* reported another NP suitable for combination therapy, an oil in water (W/O/W) double emulsion that can simultaneously contain hydrophilic and hydrophobic drugs such as DOX and erlotinib (ERL).[26] Generally, oil-in-water (O/W) NPs load hydrophobic drugs in their cores, and they are inappropriate for loading hydrophilic drugs. However, the W/O/W double emulsion has a hydrophilic core and hydrophobic layer, so it can contain both types of drugs in the same NP structure. To produce NPs with high stability, rhamnolipid, a biosurfactant with amphiphilicity, and polymers such as PLGA, Pluronic F-127, and poly (vinyl alcohol) were used. The manufactured NPs had a size of 237.7 ± 0.9 nm and was expected to have high tumor tissue accumulation through the EPR effect. The ideal ratio of the two drugs was evaluated *in vitro*, and a 1 : 1 ratio with a CI value <1 was used. SCC7 cells (2×10^6 cells) were subcutaneously inoculated into C3H/HeN mice for modeling, and each sample was intravenously injected four times over the course of a 2 day cycle. The NPs containing both drugs were 2.2 and 1.6 times more effective in tumor suppression than NPs with ERL or DOX alone, respectively, which shows the high synergistic effect of DOX and ERL and successful combination therapy using NPs.

2.3. Exosomes

Exosomes are natural NPs secreted from parental cells and have recently attracted a lot of attention as a promising drug carrier

due to their various intrinsic properties.[27] They can avoid an immune response because they are native to the human body and not a foreign material. Exosomes also contain various molecules useful for treating disease, and desirable ligands can be placed on their surfaces through genetic engineering. Recently, Wan *et al.* introduced a PEGylated exosome containing rose bengal (RB) and DOX for a combination of PDT and chemotherapy.[28] They extracted exosomes from HEK293T cells, loaded DOX and RB by sonication, and removed unloaded drugs by centrifugation. Then, they administered the exosomes to A20 cells, a B cell lymphoma cell line, and irradiated them with a 532 nm-laser for PDT. Exosomes with RB alone for PDT had a cell killing effect of a mere 28.57%, and exosomes with DOX alone for chemotherapy had an effect of 43.9%; when the two were combined, the effect increased significantly to 73.83%. In addition, Cox2 and Nox1, genes related to ferroptosis, increased by about 1.55-fold and 2.22-fold, respectively, with the combined exosome compared with the chemotherapy exosome alone group. They established a tumor model by subcutaneously injecting A20 tumor cells into the right backs of male BALB/c mice. The exosomes were i.v. injected into each mouse's tail vein every 4 days. For PDT, a 532 nm laser was used on the tumor site at a power of 0.5 W cm^{-2} for 15 minutes at 4 and 12 hours after injection of the exosomes. On the 16th day of the treatment schedule, the mice were sacrificed, the tumors were dissected, and the weights of the tumors were measured. Compared with the phosphate buffered saline (PBS) group, exosomes with chemotherapy alone suppressed the tumors by about 50%, and exosomes with PDT alone suppressed the tumors by about 55%, whereas exosomes with the combination therapy inhibited tumor growth by about 86%. Therefore, the combination of PDT and chemotherapy using an exosome carrier showed a higher therapeutic effect than that of each individual therapy.

Tumor exosomes can target homologous tumors, which is an important property. A recently published study further enhanced the homologous tumor–targeting effect of exosomes for combination therapy. Gong *et al.* noted that the properties of exosomes could be changed by the culture conditions (Fig. 3).[29] MGC803 human gastric cancer cells were exposed to various stresses (UV, low pH, heat, H_2O_2, hypoxia) to examine changes in the homologous tumor–targeting ability of exosomes secreted from them. The exosomes secreted under low-pH conditions showed the highest cellular uptake improvement compared with exosomes collected from MGC803 cells cultured in normal conditions. The cellular uptake into other normal tissue cells (NIH-3T3, GES1, and HUVEC) was not changed, indicating that the low pH treatment improved the homologous tumor–targeting ability. To prepare exosomes for combination therapy, they treated MGC803 cells with Al(III) phthalocyanine chloride tetrasulfonic acid (AP). Then, they extracted exosomes under low pH conditions and loaded them with DOX (Ex-AP-Dox). The Ex-AP-Dox exhibited rapid release of DOX upon laser irradiation due to destruction of the exosome by the photodynamic effect, which can increase the efficacy of combination therapy. The exosomes were i.v. injected into MGC803-tumor-bearing BALB/c nude mice, and tumor
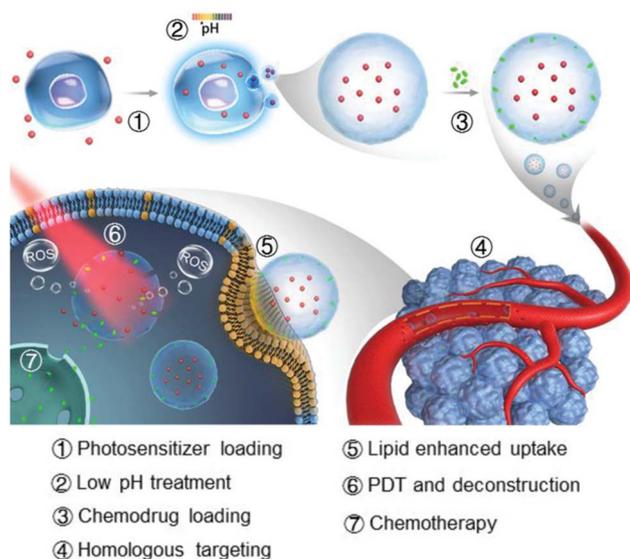
Fig. 3 Photosensitizer and DOX-loaded exosome with improved targeting to homologous tumor for simultaneous PDT and chemotherapy. Reproduced from ref. 29 with permission from [Wiley], copyright [2021].

accumulation of the exosomes was analyzed by AP fluorescence. Due to the enhanced homologous tumor–targeting, exosomes collected under low-pH conditions accumulated about 1.53 times higher in tumors than exosomes extracted under normal conditions. Additionally, biodistribution of the exosomes to other organs (heart, liver, spleen, lung, and kidney) differed little. They intravenously injected Ex-AP-Dox into MGC803 tumor-bearing mice, irradiated the tumor region with a 660 nm PDT laser, and monitored the tumor size for 26 days. Ex-AP-Dox inhibited the tumors by approximately 86%, whereas exosomes loaded with DOX alone inhibited tumors by approximately 44% compared with the PBS control group. Those results suggest that the combination of PDT and chemotherapy using exosomes was effective. Furthermore, they constructed patient-derived xenografts (PDXs) in NPG mice using cells isolated from patient-derived gastric tumor tissue. Exosomes were extracted from cells isolated from the same tissue, and in vivo therapy was performed once more in the PDX model. The Ex-AP-Dox reduced the tumor weight by 9 times compared with the free drug combination group, demonstrating the clinical potential of exosomes.

Another combination with an excellent synergistic effect is radioisotopes and chemical drugs. A study that delivered this combination in an exosome carrier was conducted by Wang et al.[30] They transfected HEK-293T cells using a lentiviral vector to introduce iRGD as an active targeting ligand at the exosome surface. The cellular uptake of the exosome was increased by the iRGD peptide, which can bind the integrin αvβ3 expressed on various tumor cells and tumor vascular cells. The iRGD-engineered exosomes (iRGD-Exo) were co-loaded with radioiodine-131 (RI-131) and DOX for combination therapy, and the final size was about 145 nm. They administered the exosome

to 8505c cells, an integrin αvβ3-positive human thyroid carcinoma, to analyse the combination effect. Cell viability after treatment with iRGD-Exo loaded with DOX or RI-131 was approximately 41 and 50%, respectively, whereas iRGD-Exo loaded with both drugs (iRGD-Exo-DOX-RI-131) reduced cell viability to 21%. To establish tumor targeting of the iRGD-Exo in vivo, they labeled the exosomes with DiR dye, i.v. injected them into 8505c tumor xenograft mice, and then detected the fluorescence using an imaging system. The iRGD-Exo signal at the tumor site 24 hours after injection was about 2.9 times stronger than the that of exosomes without iRGD. Even 96 hours after injection, iRGD-Exo-DOX-RI-131 retained 7-fold greater radioactivity than exosomes without iRGD in single photon emission computed tomography (SPECT) imaging. The maintenance of iRGD-Exo-DOX-RI-131 for a longer period can enhance the effect of the radioisotope on the tumor. They tested the antitumor efficacy with the same animal model they used to test tumor targeting. The iRGD-Exo-DOX-RI-131 reduced the tumor size by 1.95 times and the tumor weight by 2.17 times compared with the iRGD-Exo carrying RI-131 alone, indicating the usefulness of the iRGD-Exo in combination therapy with a radioisotope and chemical drug.

3. Inorganic NP-based combination therapy

3.1. Upconversion NPs (UCNPs)

UCNPs have recently been used in anticancer drugs because they can reduce off-target toxicity by controlling the release of drugs with an external light stimulus in the near-infrared (NIR) range, which has a tissue penetration depth of a few tens of millimeters.[31] The upconversion phenomenon involves multi-step absorption of low-energy photons in the NIR range and emission of multiple, narrow photoluminescence bands in the ultraviolet (UV) and visible ranges from the atomic transitions of doped atoms.[32] High-energy emitted photons specifically release the drugs conjugated to the surface of the UCNPs with photocleavable linkers.[33] Combination therapy is also achievable with UCNPs, which can also carry other prodrugs, genes, or agents for PDT (Table 3).[34] For example, Kuang et al. introduced poly-prodrug/siRNA-loaded UCNPs (PUCNP@Pt@siPLK1) with a hydrodynamic size of about 160 nm and a zeta-potential of about 10 mV. The PUCNP@Pt@siPLK1 had the capacities of trimodal theranostics: imaging and NIR light-activated release of platinum(Pt)-based drug and gene for a multifunctional antitumor therapy (Fig. 4).[35] Photoactivatable platinum(IV)-based poly-prodrugs were loaded onto the UCNPs, where they became toxic platinum(II)-based anticancer drugs upon exposure to UV-to-visible photons. The UCNPs (NaGdF$_4$:Tm^{3+}/Yb^{3+}) emit light at 350, 362, 452, and 480 nm upon irradiation with a 980 nm NIR laser, which released the platinum(IV)-based poly-prodrugs and siRNA from the UCNP surfaces. Following intracellular delivery of the PUCNP@Pt@siPlK1 to A2780 ovarian cancer cells, NIR light irradiation produced an excellent reduction of Plk1 and enhancement of cell apoptosis. In a mouse model, intratumorally injected PUCNP@Pt@siPlK1 showed multimodal

Table 3 Summary of studies employing inorganic NP in combination therapy. The tumor suppression rate was calculated as reduction of tumor size in the combination therapy group compared to the control group non-treated

| Formulation	Combination	Drug	Tumor cell (mouse)	Tumor suppression rate	Year	Ref.
Upconversion NPs	Chemotherapy/gene therapy	siPlk1/platinum(II)	A2780 (BALB/c)	96.5%	2021	35
	PDT/chemotherapy	Lapatinib/cyclometalated iridium(III)	SKOV3 (BALB/c)	80%	2020	36
	PDT/immunotherapy	Zinc phthalocyanine/Tm^{3+}-doped UCNPs/tirapazamine	B16F10 (C57BL/6J)	99%	2022	37
Plasmonic NPs	PTT/immunotherapy	Gold nanorods/FimH	4T1 (BALB/c)	99%	2022	41
	PTT/catalytic therapy/chemotherapy	Gold nanorods/indocyanine green/reduced graphene oxide/doxorubicin	HT-29 (BALB/c)	44%	2022	42
	Gene therapy/PTT/chemotherapy	Doxorubicin/Cas9/copper sulfide NPs	A375 (BALB/c)	90%	2021	43
Mesoporous silica and calcium phosphate NPs	Starvation therapy/immunotherapy	Glucose oxidase	B16F10 (C57B6)	80%	2019	46
	Chemotherapy/PTT	Doxorubicin/indocyanine green	CT26 (BALB/c)	90%	2020	47
	PTT/immunotherapy	Polydopamine/ovalbumin	B16-OVA (C57BL/6)	99%	2021	48
	Chemodynamic therapy/starvation therapy	Glucose oxidase/Cu^{2+} ion/doxorubicin	4T1 (BALB/c)	93%	2021	52
	Chemodynamic therapy/PDT/starvation therapy	Glucose oxidase/Mn^{2+} ion/sinoporphyrin sodium	4T1 (BALB/c)	99%	2021	54
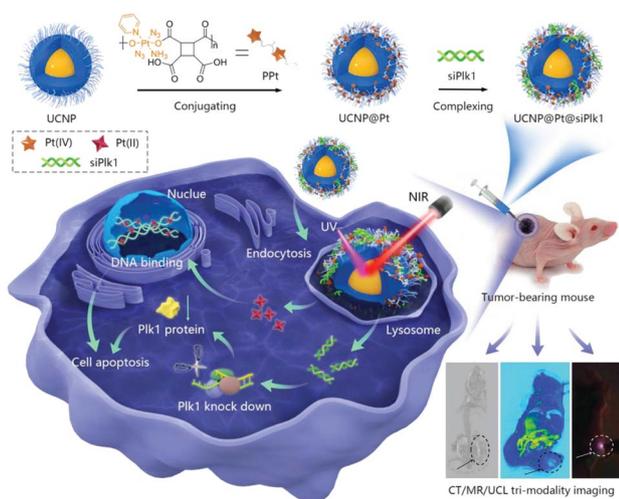
Fig. 4 NIR-triggered poly-prodrug/siRNA delivery through upconversion NPs for synergistic cancer therapy. Reproduced from ref. 35 with permission from [Wiley], copyright [2021].

cancer therapeutic capabilities, including tumor growth suppression from the activated Pt-based drugs and Plk1 knockdown from the released siRNA. Moreover, no noticeable organ accumulation of platinum or change in body weight was observed.

To induce the specific targeting ability of UCNP-based anticancer drug delivery vehicles, Zhao *et al.* reported the use of lapatinib-functionalized photosensitizing complexes and NaYF$_4$:Yb/Tm@NaYF$_4$ UCNPs co-loaded with polymeric micelles (PolyIrLa).[36] Cyclo-metalated iridium(III) complexes were conjugated with PEG to improve their water solubility, and the UCNPs were embedded in the micelle for NIR-triggered PDT. The encapsulated UCNPs exhibited a high extinction coefficient for NIR light and emitted UV and blue light, which excited the iridium(III) complexes to produce ROS. Because iridium(III) complexes have toxicity in the dark, the specific targeting ability of the lapatinib-conjugated nanomedicine is important for reducing off-target cytotoxicity. Moreover, lapatinib is a dual tyrosine kinase inhibitor for the human EGFR2 and HER2/neu pathways. The PolyIrLa had a hydrodynamic size of ~168 nm and ROS generation capability under 980 nm NIR laser irradiation. Given its ROS generation and specific targeting abilities, the PolyIrLa showed an excellent cell apoptosis effect under NIR irradiation and depletion of HER2 activity in SKOV3 cells. An i.v. injection of PolyIrLa in SKOV3 tumor-bearing mice produced better inhibition of tumor growth than the non-targeted PolyIr (without lapatinib), indicating that the combination of PDT and lapatinib was effective.

Wu *et al.* introduced a combined cancer therapy platform that loaded zinc phthalocyanine (ZnPc) and TPZ for PDT onto silica yolk–shelled UCNPs (UCNP-YS@ZnPc@TPZ) and then added an optogenetically engineered bacterium.[37] The NaYF$_4$:Yb/Tm/Nd@NaYF$_4$:Nd UCNPs showed both blue and red photoluminescence (PL) under 808 nm NIR irradiation. Because the red PL of the UCNPs can excite the photosensitizer, ZnPc, the UCNP-YS@ZnPc@TPZ were able to generate ROS under NIR irradiation. The blue PL of the UCNPs induced the expression of IFN-γ from the light-regulated pDawn plasmid-engineered bacterium. To secure the viability of the engineered bacteria,

the UCNP-YS@ZnPc@TPZ and bacteria were co-encapsulated with chitosan, which can swell in acidic conditions. In a hypoxic environment, hydroxyl radicals from TPZ can enhance PDT efficiency. Upon treatment with those components, primary tumor apoptosis occurred with PDT from ZnPc, and TPZ presented tumor-associated antigens to the immune system to activate immunogenic cell death. The flow cytometry data from a B16F10-xenografted mouse model show that orally delivered UCNP-YS@ZnPc@TPZ and bacteria caused significant increase in $CD4^+$ and $CD8^+$ T cells. The combination of PDT and immunotherapy using UCNP-YS@ZnPc@TPZ was verified in cultured B16F10 cells and mouse models, showing the highest reduction in the density of tumor cells among groups without a significant accumulation of NPs or body weight loss.

3.2. Plasmonic NPs

Plasmonic NPs can effectively emit heat that originates from the collective oscillation of electrons excited by external light.[38] The peak wavelengths of light that interact with plasmonic NPs can easily be tuned using different sizes or materials for the NPs.[39] For example, gold NPs or copper sulfide (CuS) NPs can be used for heat conversion and photothermal therapy (PTT).[40] When those NPs are delivered, a combination cancer therapy that includes PTT, chemotherapy, and immunotherapy can be administered. Additionally, anticancer therapy activated by external stimuli can lower off-target cytotoxicity. Recently, Hwang et al. introduced synergistic anticancer plasmonic NPs for PTT and immunotherapy.[41] To produce Escherichia coli (E. coli) mimetic (ECA) gold nanorods (AuNRs), the AuNRs were coated with lipids and membrane proteins extracted from E. coli and functionalized with FimH, which can target a specific N-glycan on epithelial tissue. The ECA showed a hydrodynamic size of ∼117 nm and a zeta-potential value of −12.7 mV. ECA induced apoptotic death in CT-26 cells both in vitro and in vivo in mouse models under NIR (808 nm) illumination. When the ECA was i.v. injected into mice, no noticeable tumor growth and an enhanced survival rate (∼100%) were observed. After PTT under NIR irradiation, the maturation of dendritic cells (DCs) was observed in the lymph nodes because of the apoptotic bodies and FimH taken up by the DCs. After a first immunotherapy treatment, ECA with NIR irradiation effectively inhibited a second cancer challenge of CT-26 lung metastatic and 4T1 breast cancer in a mouse model. Upon NIR irradiation, ECA also induced CT-26 tumor antigen-specific T-cell immunity and the expression of IFN-γ and TNF-α, which protected the mice from cancer metastasis. Therefore, ECA can inhibit metastasis and tumor recurrence after primary tumor treatment via PTT and activation of the immune system.

Maji et al. reported a triple combination of catalytic therapy, PTT, and chemotherapy using DOX, reduced graphene oxide (rGO), and indocyanine green (ICG) loaded onto AuNRs (GNR-ICG@rGO-DOX) (Fig. 5).[42] They prepared PEG and a mesoporous silica coating on AuNRs containing ICG and DOX at the surface. Peroxidase activity from the rGO in the GNR-ICG@rGO-DOX was confirmed by measuring ROS generation. Under 808 nm NIR irradiation, efficient heat conversion from both the
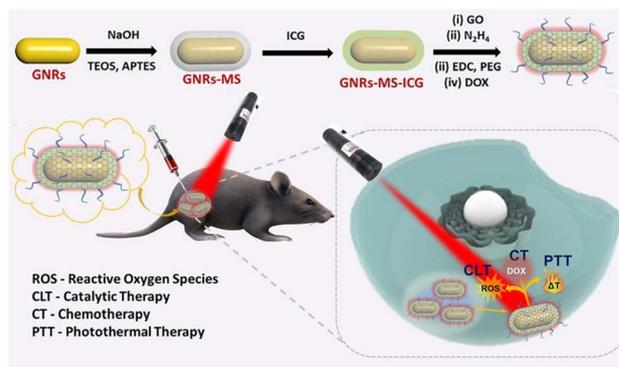

Fig. 5 Rationally designed plasmonic NP-mediated trimodal (catalytic-, chemo-, and photothermal-) therapy against cancer. Reproduced from ref. 42 with permission from [American chemical Society], copyright [2022].

ICG and AuNRs increased cytotoxicity compared with the control. Because only the ICG molecules have a rapid clearance rate in vivo and a low extinction coefficient in the NIR range, Maji et al. claimed that the GNR-ICG@rGO-DOX should show the highest heat conversion efficiency among the samples they tested. The DOX release kinetics profile was confirmed by a positive correlation with acidic pH conditions. Upon 808 nm NIR laser irradiation, successful anticancer therapy with the GNR-ICG@rGO-DOX were observed in HT-29 cells and HT-29 tumor-bearing mice that received a peritumoral injection.

Chen et al. demonstrated the usefulness of plasmonic NPs in gene therapy with CRISPR-Cas9 gene editing.[43] They used external stimuli-responsive methods to enable stimulus-sensitive activatable CRISPR-Cas9 complexes (RNPs). The complexes were loaded onto the surfaces of CuS NPs by surface-coating complementary DNA sequences onto sgRNA, which can be heated by an NIR light source. They synthesized CuS-RNP/DOX@PEI by intercalating DOX between the DNA molecules on CuS NPs and sgRNA using the electrostatic interaction between the CuS-RNP/DOX and PEI. At the first 808 nm irradiation, the endosomal escape capability released not only the Cas9 RNP into the cytosol to knock out the target gene, but also the DOX for chemotherapy. Then, the second irradiation induced PTT to reduce tumor thermotolerance. Chen et al. confirmed the synergistic effects of CuS-RNP/DOX@PEI using A375 tumor-bearing mice, showing reduction in cell density and expression of Hsp90α, which is the target of the Cas9 RNP. The tumor volume of the mouse model significantly decreased under NIR irradiation following intratumoral injection of the CuS-RNP/DOX@PEI. Overall, their therapeutic nanocomplexes showed excellent antitumor efficacy by combining gene therapy, PTT, and chemotherapy.

3.3. Mesoporous silica and calcium phosphate NPs

Mesoporous silica NPs (MSNs) are silica-based, few hundred nanometer-sized, porous NPs with well-defined porosity and morphology. Their surface chemistry and size can easily be tuned, resulting in a high drug-loading capacity and surface

functionalization for various biomedical applications.[44] For combined cancer treatment and imaging, the surfaces of MSNs containing imaging agents, anticancer drugs, and enzymes can be decorated with immune-stimulating antigens.[45] In most cases, the biocompatibility and low cytotoxicity of silica materials are advantages for biomedical applications.

Xie *et al.* reported a GOx-loaded MSN-mediated combination therapy.[46] For starvation- and immuno-combination therapy, B16F10 melanoma cancer cell membrane was extracted, and the surfaces of GOx-loaded MSNs were coated with lipids and proteins from those cell membrane extracts, which produced a hydrodynamic size of about 100 nm (CMSN-GOx) and camouflaged the particles from immune cells. Xie *et al.* claimed that GOx was delivered safely to a xenografted tumor site *via* passive and active targeting after an i.v. injection of CMSN-GOx. After GOx delivery, the apoptosis of cancer cells was induced, resulting in antigen presentation to DCs. In conjunction with CMSN-GOx, PD-1 was also administered as an adjuvant to enhance DC maturation and immunotherapy efficacy through recruited effector T cells. Starvation therapy efficacy was evaluated by measuring [^{18}F] 2-fluoro-2-deoxy-D-glucose level in positron emission tomography. CMSN-GOx with PD-1 treatment showed the highest tumor therapy efficiency. Based on the flow cytometry results, the effective T cell ratio (CD4+ T cells, CD8+ T cells, CD8+ T_{eff}-to-T_{reg} ratio, and CD4+ T_{eff}-to-T_{reg} ratio) increased, presumably through enhanced DC maturation. This combination therapy successfully decreased the tumor volume in a mouse model and produced the highest survival rate among the sample groups, including CMSN-GOx or PD-1 alone.

Zhang *et al.* reported a chemo-photothermal cancer therapy using MSNs with anticancer drugs and gas-producing agents.[47] For their combination therapy, they loaded ammonium bicarbonate (NH$_4$HCO$_3$, ABC), ICG, and DOX into the pores of MSNs. A polydopamine (PDA) coating was used to encapsulate all the molecules inside the pores of the MSNs. To provide colloidal stability and intracellular deliverability, PEG and cyclic cell-penetrating peptides (RGDs) were functionalized on the MSN surfaces (M(abc)-DOX@PDA-ICG-PEG-RGD). The MSNs showed a hydrodynamic size of ~260 nm and a negatively charged surface (zeta potential: −19 mV). After intracellular delivery of the MSNs, photothermal conversion from ICG and PDA induced the generation of CO$_2$ gas and ammonia, which disrupted the PDA layer of the MSNs upon irradiation with an 808 nm NIR laser. DOX was efficiently and controllably delivered into tumor cytosol in a mouse model. The MSNs might have accumulated on the tumor after i.v. injection through passive targeting. Heat conversion and DOX release were confirmed using both cultured cell levels and mouse models. The delivery efficiency of DOX *in vivo* was highest when both MSNs and NIR treatment were used. Among the samples tested, the MSNs showed the highest antitumor growth inhibition without causing any abrupt body weight changes in the mouse model.

In 2021, Huang *et al.* introduced PDA- and ovalbumin-coated MSN (MSN-ABC@PDA-OVA) nanovaccines for photothermal-immunotherapy in a melanoma-xenografted mouse model (Fig. 6).[48] Because PDA can itself be used as a photothermal conversion agent, the PDA surface coating was paired with ABC

as a gas-forming agent under NIR irradiation, in a manner similar to the previous work. After degradation of the PDA layer, OVA was released to induce DC maturation, which resulted in the activation of effector T cells. Upon NIR irradiation, heat conversion and OVA release efficiency of the MSN-ABC@PDA-OVA were confirmed in *ex vivo* cultured cells and *in vivo* mouse models. Cy7 labeled OVAs were accumulated effectively on the nearest lymph nodes from the injection site with NIR laser treatment, meaning the NIR-dependent antigen presentation ability of the MSNs. B16-OVA tumor-xenografted mouse model was used for confirming the efficacy of the photothermal-immunotherapy. Intratumorally injected MSN-ABC@PDA-OVA showed activation of antigen-specific CD8+ and CD4+ T cells. The highest antitumor effects and survival rates were confirmed under treatment with both the MSN-ABC@PDA-OVA and NIR irradiation. After the first MSN injection, the B16-OVA tumor was re-inoculated to assess tumor metastasis and memory efficacy in the mouse model. No significant increase in the re-challenged tumor volume and the highest survival rate were observed under treatment with both MSN-ABC@PDA-OVA and NIR irradiation, and a significant increase of CD4+ effector memory T cells was confirmed. These results indicate that memory immunity effectively inhibited cancer recurrence and metastasis in the mouse model after treatment with this MSN combination therapy.

Calcium phosphate (CaP) NPs are biodegradable, biocompatible, and biomimetic inorganic nanomaterials.[49] CaPs loaded with multiple drugs have been used for combination cancer therapy.[50] Their synthesis and functionalization are simple at a mild reaction temperature range (from r.t. to 37 °C), resulting in a high loading efficiency of various enzymes and drugs. Fu *et al.* reported a starvation-gas cancer therapy using GOx and L-arginine (L-Arg) co-loaded CaPs.[51] These CaPs were furthered functionalized with hyaluronic acid (GCAH) that can target a CD44 overexpressed tumor. After the starvation therapy through the glucose oxidation by GOx, H$_2$O$_2$ molecules are
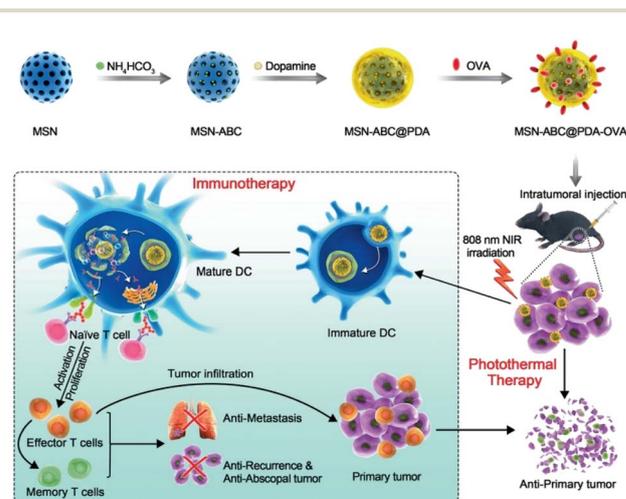

Fig. 6 Mesoporous silica NP-based nanovaccine for photothermal-immunotherapy against melanoma. Reproduced from ref. 48 with permission from [Wiley], copyright [2021].

produced as products that are used as reactant for the nitric oxide (NO) generation. Controlled release of NO can be used as a gas cancer therapy agent by converting ROS to more toxic anions. After i.v. injection of GCAH for three times in two weeks, a tumor growth of the GCAH treated group was suppressed by about 80% compared to the control group. Even with the negatively charged surface, GCAH were successfully delivered the 4T1 tumor bearing BALB/c mouse, probably due to both the CD44 active and passive targeting. Biocompatible cation-doped CaP were also developed by the same group for a chemo-dynamic-starvation[52,53] and a PDT-chemodynamic-starvation cancer therapy.[54]

4. Conclusion and outlook

In this review, we summarized recent studies about nanomedicines for combination cancer therapy. Although traditional chemotherapy is being widely used to treat cancer, nanomedicines composed of organic and inorganic nanomaterials are being recognized as new anticancer drugs or therapeutic platforms for *in vivo* systems because of their unique advantages, such as long circulation times, low off-target cytotoxicity, high heat conversion efficiency, external-stimulus-sensitive drug activity, deep penetration, and high intracellular delivery efficiency.[55] Nonetheless, before they can be used clinically, remaining concerns about safety issues (acute toxicity, chronic toxicity, and immune response), biodegradability, mass production, reproducibility, heterogeneity between nanomedicines and different batches, and toxicity evaluation in cells, organoids, and animal models should be thoroughly addressed and investigated.[56] In general, the biocompatibility of inorganic nanomaterials is not understood as fully as that of organic nanomaterials. For that reason, only a few inorganic nanomaterials have been approved by the FDA, whereas many organic nanomaterials are being approved.[57] Nevertheless, selectively combining multiple anticancer therapeutic strategies using the advantages of both organic and inorganic NPs could offer potential synergy that could be beneficial in treating drug-resistant tumor cells and tissues.[58] When researchers design nanomedicines for cancer therapy, they might need to not only take advantage of the strengths of inorganic nanomaterials (high stability and heat conversion efficiency) and organic nanomaterials (low cytotoxicity and biodegradability), but also strike a balance between them. Therefore, we expect emerging organic and inorganic nanomedicines to be important parts of the next generation of anticancer treatments that will be widely applied in human patients in the future.

Conflicts of interest

The authors declare no conflict of interest.

Acknowledgements

References

1 A. M. Vargason, A. C. Anselmo and S. Mitragotri, *Nat. Biomed. Eng.*, 2021, **5**, 951–967.

2 M. J. Mitchell, M. M. Billingsley, R. M. Haley, M. E. Wechsler, N. A. Peppas and R. Langer, *Nat. Rev. Drug Discovery*, 2021, **20**, 101–124.

3 X. Huang, N. Kong, X. Zhang, Y. Cao, R. Langer and W. Tao, *Nat. Med.*, 2022, **28**, 2273–2287.

4 H. Maeda, J. Wu, T. Sawa, Y. Matsumura and K. Hori, *J. Controlled Release*, 2000, **65**, 271–284.

5 J. Yoo, C. Park, G. Yi, D. Lee and H. Koo, *Cancers*, 2019, **11**, 640.

6 J. Son, G. Yi, J. Yoo, C. Park, H. Koo and H. S. Choi, *Adv. Drug Delivery Rev.*, 2019, **138**, 133–147.

7 J. Shi, P. W. Kantoff, R. Wooster and O. C. Farokhzad, *Nat. Rev. Cancer*, 2016, **17**, 20.

8 R. A. Petros and J. M. DeSimone, *Nat. Rev. Drug Discovery*, 2010, **9**, 615–627.

9 M. Ramachandran, Z. Ma, K. Lin, C. De Souza and Y. Li, *Nanoscale Adv.*, 2022, **4**, 4470–4480.

10 S. Rawal and M. M. Patel, *J. Controlled Release*, 2019, **301**, 76–109.

11 T. Lammers, V. Subr, K. Ulbrich, W. E. Hennink, G. Storm and F. Kiessling, *Nano Today*, 2010, **5**, 197–212.

12 V. P. Torchilin, *Nat. Rev. Drug Discovery*, 2005, **4**, 145–160.

13 E. Park, D. Lee, Y. Lee, E. Jeong, S. Kim and H. Koo, *Colloid Interface Sci. Commun.*, 2022, **46**, 100565.

14 M. Wu, Q. Wang, S. Chen, Z. Zhou, J. Li, H. Sun, J. Liu, G. Wang, F. Zhou and M. Sun, *J. Controlled Release*, 2022, **350**, 1–10.

15 X. Hou, T. Zaks, R. Langer and Y. Dong, *Nat. Rev. Mater.*, 2021, **6**, 1078–1094.

16 D. Zhang, G. Wang, X. Yu, T. Wei, L. Farbiak, L. T. Johnson, A. M. Taylor, J. Xu, Y. Hong, H. Zhu and D. J. Siegwart, *Nat. Nanotechnol.*, 2022, **17**, 777–787.

17 W. H. Lee, J. G. Rho, Y. Yang, S. Lee, S. Kweon, H.-M. Kim, J. Yoon, H. Choi, E. Lee, S. H. Kim, S. You, Y. Song, Y. S. Oh, H. Kim, H. S. Han, J. H. Han, M. Jung, Y. H. Park, Y. S. Choi, S. Han, J. Lee, S. Choi, J.-W. Kim, J. H. Park, E. K. Lee, W. K. Song, E. Kim and W. Kim, *ACS Nano*, 2022, **16**, 20057–20074.

18 Y. Lee, K. Sugihara, M. G. Gillilland, S. Jon, N. Kamada and J. J. Moon, *Nat. Mater.*, 2020, **19**, 118–126.

19 Y. Bae and K. Kataoka, *Adv. Drug Delivery Rev.*, 2009, **61**, 768–784.

20 S. Wang, J. Lin, Z. Wang, Z. Zhou, R. Bai, N. Lu, Y. Liu, X. Fu, O. Jacobson, W. Fan, J. Qu, S. Chen, T. Wang, P. Huang and X. Chen, *Adv. Mater.*, 2017, **29**, 1701013.

21 C. Qi, L.-H. Fu, H. Xu, T.-F. Wang, J. Lin and P. Huang, *Sci. China: Chem.*, 2019, **62**, 162–188.

22 Y. Tian, M. R. Younis, Y. Tang, X. Liao, G. He, S. Wang, Z. Teng, P. Huang, L. Zhang and G. Lu, *J. Nanobiotechnol.*, 2021, **19**, 365.

23 J. Wu, Y. Zhang, K. Jiang, X. Wang, N. T. Blum, J. Zhang, S. Jiang, J. Lin and P. Huang, *Adv. Mater.*, 2022, **34**, 2200062.

24 D. Lee, S.-y. Jang, S. Kwon, Y. Lee, E. Park and H. Koo, *ACS Appl. Mater. Interfaces*, 2021, **13**, 10812–10821.

25 Q. Liu, T.-X. Zhang, Y. Zheng, C. Wang, Z. Kang, Y. Zhao, J. Chai, H.-B. Li, D.-S. Guo, Y. Liu and L. Shi, *Small*, 2021, **17**, 2006223.

26 Y. Lee, D. Lee, E. Park, S.-y. Jang, S. Y. Cheon, S. Han and H. Koo, *J. Nanobiotechnol.*, 2021, **19**, 411.

27 S. Fu, Y. Wang, X. Xia and J. C. Zheng, *NanoImpact*, 2020, **20**, 100261.

28 Z. Wan, X. Gan, R. Mei, J. Du, W. Fan, M. Wei, G. Yang, W. Qin, Z. Zhu and L. Liu, *J. Nanobiotechnol.*, 2022, **20**, 385.

29 C. Gong, X. Zhang, M. Shi, F. Li, S. Wang, Y. Wang, Y. Wang, W. Wei and G. Ma, *Adv. Sci.*, 2021, **8**, 2002787.

30 C. Wang, N. Li, Y. Li, S. Hou, W. Zhang, Z. Meng, S. Wang, Q. Jia, J. Tan, R. Wang and R. Zhang, *J. Nanobiotechnol.*, 2022, **20**, 247.

31 H. Kim, K. Chung, S. Lee, D. H. Kim and H. Lee, *Wiley Interdiscip. Rev.: Nanomed. Nanobiotechnol.*, 2016, **8**, 23–45.

32 Y. Wang, S. Song, S. Zhang and H. Zhang, *Nano Today*, 2019, **25**, 38–67.

33 J. F.-C. Loo, Y.-H. Chien, F. Yin, S.-K. Kong, H.-P. Ho and K.-T. Yong, *Coord. Chem. Rev.*, 2019, **400**, 213042.

34 Y.-Q. Liu, L.-Y. Qin, H.-J. Li, Y.-X. Wang, R. Zhang, J.-M. Shi, J.-H. Wu, G.-X. Dong and P. Zhou, *Nanomedicine*, 2021, **16**, 2207–2242.

35 G. Kuang, H. Lu, S. He, H. Xiong, J. Yu, Q. Zhang and Y. Huang, *Adv. Healthcare Mater.*, 2021, **10**, 2100938.

36 J. Zhao, X. Zhang, L. Fang, C. Gao, C. Xu and S. Gou, *Small*, 2020, **16**, 2000363.

37 C. Wu, M. Cui, L. Cai, C. Chen, X. Zhu, Y. Wu, J. Liu, H. Wang and Y. Zhang, *ACS Appl. Mater. Interfaces*, 2022, **14**, 13094–13106.

38 M. Sharifi, F. Attar, A. A. Saboury, K. Akhtari, N. Hooshmand, A. Hasan, M. A. El-Sayed and M. Falahati, *J. Controlled Release*, 2019, **311–312**, 170–189.

39 S. Hwang, J. Nam, S. Jung, J. Song, H. Doh and S. Kim, *Nanomedicine*, 2014, **9**, 2003–2022.

40 J. Fang and Y.-C. Chen, *Curr. Pharm. Des.*, 2013, **19**, 6622–6634.

41 J. Hwang, E.-K. An, S.-J. Kim, W. Zhang and J.-O. Jin, *ACS Nano*, 2022, **16**, 8472–8483.

42 S. K. Maji, S. Yu, E. Choi, J. W. Lim, D. Jang, G.-y. Kim, S. Kim, H. Lee and D. H. Kim, *ACS Omega*, 2022, 7, 15186–15199.

43 C. Chen, Y. Ma, S. Du, Y. Wu, P. Shen, T. Yan, X. Li, Y. Song, Z. Zha and X. Han, *Small*, 2021, **17**, 2101155.

44 W. Q. Lim, S. Z. F. Phua, H. V. Xu, S. Sreejith and Y. Zhao, *Nanoscale*, 2016, **8**, 12510–12519.

45 R. Huang, Y.-W. Shen, Y.-Y. Guan, Y.-X. Jiang, Y. Wu, K. Rahman, L.-J. Zhang, H.-J. Liu and X. Luan, *Acta Biomater.*, 2020, **116**, 1–15.

46 W. Xie, W.-W. Deng, M. Zan, L. Rao, G.-T. Yu, D.-M. Zhu, W.-T. Wu, B. Chen, L.-W. Ji, L. Chen, K. Liu, S.-S. Guo, H.-M. Huang, W.-F. Zhang, X. Zhao, Y. Yuan, W. Dong, Z.-J. Sun and W. Liu, *ACS Nano*, 2019, **13**, 2849–2857.

47 Z. Zhang, L. Zhang, C. Huang, Q. Guo, Y. Zuo, N. Wang, X. Jin, L. Zhang and D. Zhu, *Biomater. Sci.*, 2020, **8**, 6754–6763.

48 C. Huang, L. Zhang, Q. Guo, Y. Zuo, N. Wang, H. Wang, D. Kong, D. Zhu and L. Zhang, *Adv. Funct. Mater.*, 2021, **31**, 2010637.

49 C. Qi, J. Lin, L.-H. Fu and P. Huang, *Chem. Soc. Rev.*, 2018, **47**, 357–403.

50 L.-H. Fu, Y.-R. Hu, C. Qi, T. He, S. Jiang, C. Jiang, J. He, J. Qu, J. Lin and P. Huang, *ACS Nano*, 2019, **13**, 13985–13994.

51 L.-H. Fu, C. Li, W. Yin, Y.-R. Hu, T. Sun, Y. Wan, J. Lin, Z. Li and P. Huang, *Adv. Healthcare Mater.*, 2021, **10**, 2170110.

52 L.-H. Fu, Y. Wan, C. Qi, J. He, C. Li, C. Yang, H. Xu, J. Lin and P. Huang, *Adv. Mater.*, 2021, **33**, 2006892.

53 C. Li, Y. Wan, Y. Zhang, L.-H. Fu, N. T. Blum, R. Cui, B. Wu, R. Zheng, J. Lin, Z. Li and P. Huang, *Adv. Mater.*, 2022, **34**, 2103980.

54 L.-H. Fu, Y. Wan, C. Li, C. Qi, T. He, C. Yang, Y. Zhang, J. Lin and P. Huang, *Adv. Funct. Mater.*, 2021, **31**, 2009848.

55 W. Fan, B. Yung, P. Huang and X. Chen, *Chem. Rev.*, 2017, **117**, 13566–13638.

56 D. C. Manatunga, V. U. Godakanda, R. M. de Silva and K. M. N. de Silva, *Wiley Interdiscip. Rev.: Nanomed. Nanobiotechnol.*, 2020, **12**, e1605.

57 J. Nam, S. Son, K. S. Park, W. Zou, L. D. Shea and J. J. Moon, *Nat. Rev. Mater.*, 2019, **4**, 398–414.

58 S. Vinogradov and X. Wei, *Nanomedicine*, 2012, **7**, 597–615.